阪神高速道路公団
技報第13号 1993

平成4年度 土木学会田中賞（論文部門）受賞の『長大斜張橋の構造形式選定と耐震耐風設計技術の開発』のうちの主論文

Earthquake-resistant and wind-resistant design of the Higashi-Kobe Bridge

Y. Yamada[a], N. Shiraishi[a], K. Toki[b], M. Matsumoto[a], K. Matsuhashi[c], M. Kitazawa[c] and H. Ishizaki[c]

[a] *Department of Civil Engineering, Kyoto University, Kyoto, Japan*
[b] *Disaster Prevention Research Institute, Kyoto University, Uji, Japan*
[c] *Hanshin Expressway Public Corporation, Chuo-ku, Osaka, Japan*

Abstract

The Higashi-Kobe Bridge is a long-span cable-stayed bridge in which the unique feature is that the main girder is supported by towers and piers in such a way that the girder is movable in the longitudinal direction. This supporting method was adopted with the aim of lengthening the fundamental period of the bridge to a relatively longer period. By using this supporting method, the effects of the inertial forces due to the superstructure on the bridge towers and the caisson foundations will be greatly reduced, thereby resulting in a more rational and economical bridge design. On the other hand, various special considerations had to be taken in the wind-resistant design of the tower frames in which two elegantly projecting columns are tied at relatively lower position for aesthetic reason. Corner-cut scheme has been adopted to counter galloping. Mechanism of rain-wind induced vibration in cables was investigated; and as a countermeasure to this, cables with gear-like section was developed and is the first in the world to be used in cable-stayed bridges.

1. OUTLINE OF THE HIGASHI-KOBE BRIDGE

The Higashi-Kobe bridge, a steel cable-stayed bridge presently under construction, is one of the several large-scale bridges that will form the Osaka Bay Route of the Hanshin Expressway Public Corporation. The features of this bridge (Figure 1) can be summarized as follows:

- Center span length: 485m
- Width of bridge: 13.5m (3 lanes each for upper and lower decks)
- Main girder: 9m high Warren truss with no vertical chords
- Tower: H-shaped tower with 146.5m high columns and curved cross beams tied at relatively low positions
- Cable: Double-plane multiple cable system with harp pattern arrangement
- Floor system: Steel deck composite with the main girder truss

- Foundations: Pneumatic caissons for the towers (L×B×H=32×35×25m);
  Cast-in-place piles for the end piers and the pendulum piers.

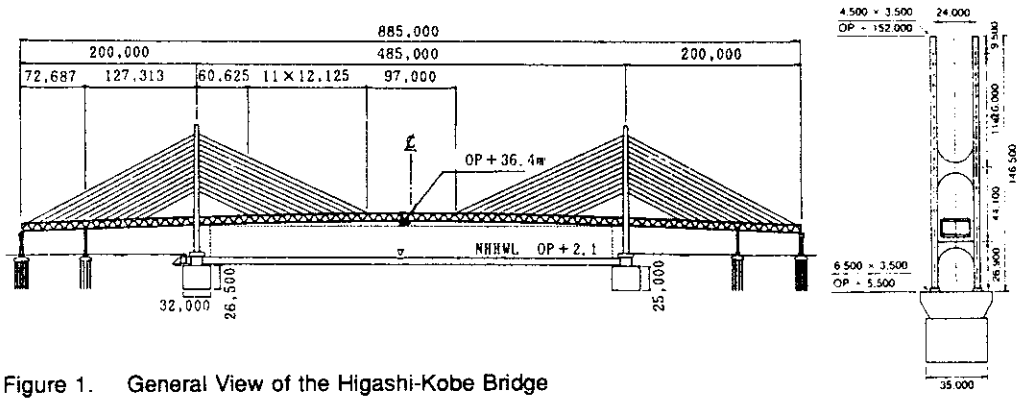

Figure 1. General View of the Higashi-Kobe Bridge

2. EARTHQUAKE-RESISTANT DESIGN OF HIGASHI-KOBE BRIDGE

2.1. General Concepts of Aseismic Design of Higashi-Kobe Bridge

Upon completion, the Higashi-Kobe Bridge will be one of the longest cable-stayed bridges in Japan. Because of high seismicity in Japan, earthquake-resistant design of the bridge is a critical issue in the general design process of the bridge. Cable-stayed bridges are so highly redundant (statically indeterminate) that sophisticated computer analysis is needed. General concepts of the aseismic design are given as follows:

- Keep the bridge structure flexible to a reasonable level in order to reduce seismic inertia, but provide safety devices to suppress excessive deformation.
- Adopt multi-mode response analysis to determine sectional forces due to the design earthquake loads in order to properly model the bridge behavior.

2.2. Selection of the Basic Structural Configuration

In order to determine the ideal support system for the Higashi-Kobe Bridge, the earthquake response of several configurations of structural system were considered and the comparison is shown in Table 1.

The advantages and disadvantages of these supporting systems can be summarized as follows:

- The use of one fixing support or two fixing supports, case 1 and case 5 in Table 1, causes large forces in the fixed piers. And, even multiple fixing support system (case 2), cannot disperse earthquake forces.
- The use of elastic supports (case 3) makes it possible to adjust natural period of the bridge adequately enough to reduce earthquake forces in the towers. However, using such system will require careful maintenance.
- The use of all movable supports (case 4) where the main girder is supported by towers via cables (herein refered to as "all free") gives the bridge a rather longer natural period, and therefore reduces earthquake forces of the tower considerably. However, the displacement of the main girder can be quite large.

Acceleration response spectrum for the superstructure design was determined against the most unfavorable case at the construction site especially in the longer period range. Table 2 shows forces and displacements categorized according to design loads. Adopting the all-

free support system, wind loads (rather than earthquake loads) governed in the design of the towers. As a result, the size of the caisson for the all-free system can be made about 10m smaller than that designed for a two-fixed support system.

Table 1 Comparison of different supporting systems

Support Configuration	Natural Period *sec.*	Section Forces (tower base) *kN, kN-m*	Displacement (girder) *cm*
(1). Two Supports Fixed *M+F+F+M*	1.42	M=608000 N=90000 S=24000	20
(2). All Supports Fixed *F+F+F+F*	1.26	M=609000 N=85000 S=24000	18
(3). Spring Supports *M+S+S+M*	3.01	M=308000 N=88000 S=10000	37
(4). Supports All Free *M+M+M+M*	8.69	M=155000 N=90000 S= 2000	56
(5). One Support Fixed *M+F+M+M*	2.21	M=602000 N=97000 S=23000	22

N.B. – Load combination: $D + L_{EQ} + EQ_L + T_{15}$
– Fan pattern cable arrangement is assumed
– Design Spectrum for Ajigawa Bridge is used
– Forces are given per column
– 'M' movable; 'F' fixed; 'S' elastic

Table 2. Forces and Displacements by design Loads

	Tower base force and girder displacement			
	All Free		Two Fixing System	
	S (kN)	M (kN*m)	S (kN)	M (kN*m)
W	9200	440000	9300	219000
EQ	7600	406000	25000	600000
Critical Design load	7200	348000	22900	400000
	$(D + W + T)/1.35$		$(D + L + EQ + T)/1.50$	
Plate Thickness at Tower Base	36mm		45mm	
Caisson Size (L×B)	32m × 35m		40m × 35m	

N.B. – Harp pattern cable arrangement is assumed
– Forces are given per column

2.3. Countermeasures for Large Displacements

Having selected the all-free configuration, the following problems should be properly addressed:

- accurate and reliable evaluation of the earthquake response of long-period structure;
- disadvantage due to out-of-plane buckling of the tower column not fixed to the main girder;

• large longitudinal displacement of the main girder due to earthquake and wind.

The latter two problems can be solved by arranging the cables in a harp pattern. Arranging cables in harp pattern has the effect of constraining rotational movement of the towers and also of constraining longitudinal movement of the girder (Figure 2). The remaining part of this paper addresses the first stated problem.

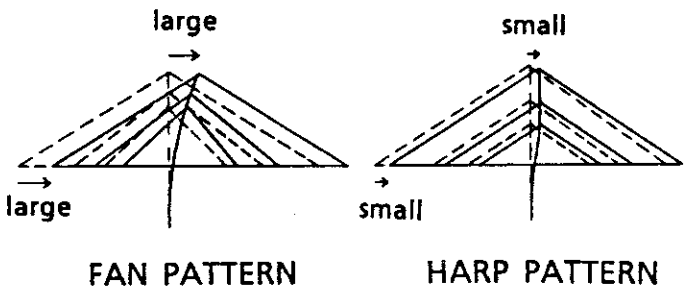

Tower Displacement in cm.

Pattern	HARP	FAN
WIND	61.3	189.5
SEISMIC	62.3	75.5

Figure 2. Displacements of Fan and Harp Cable Pattern

2.4. Design Acceleration Response Spectra

The design spectrum was provided with a relatively large safety margin in the long period range. This is because the Higashi-Kobe bridge has an unprecedented long natural period of longitudinal sway mode oscillation. The design spectrum range around the natural period plays a critical role in determining the structure response to earthquakes. The design spectrum was determined by the following procedure:

1. In formulating the design acceleration response spectrum, a 1000 meter deep bedrock at the construction site was assumed from the fact that a granite layer lies at that depth. By taking the deep bedrock, there occurs a possibility of the seismic wave and bridge oscillation frequencies coinciding and causing amplification in the long period range. The bedrock was assumed to be somewhat deeper than usual to increase the safety margin.
2. The maximum acceleration of seismic waves at the bedrock was assumed to be 160 gal as an expected value during a 100-year return period. For the input waves W1 at the bedrock, three earthquake records including Taft were used as data which were reliable up to the range of 0.07 Hz. These are then converted to their equivalent bedrock motion (Figure 3).
3. Waves W2 at the 80m deep design ground base, which will be used for the earthquake response analysis using finite element method, were obtained by multiple wave reflection analysis in which strain dependency of soil properties was considered (Figure 4).
4. The acceleration response spectra for the superstructure were obtained from the tower base waves W3 in the above analysis in which the superstructure, substructure and the surrounding ground are modeled. These spectra have peaks at natural periods of the ground coinciding with that of the bridge.
5. The design spectrum was determined by taking an envelope curve of mean spectrum of these three in longer period range. The shorter and intermediate part of the spectrum was determined by refering to the specifications for highway bridges in Japan and other standards for bridges (Figure 5).

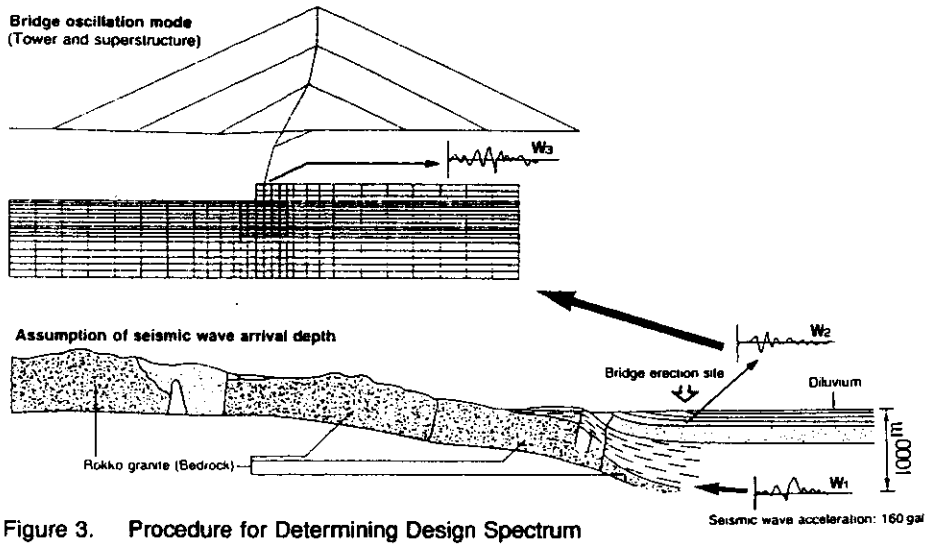

Figure 3. Procedure for Determining Design Spectrum

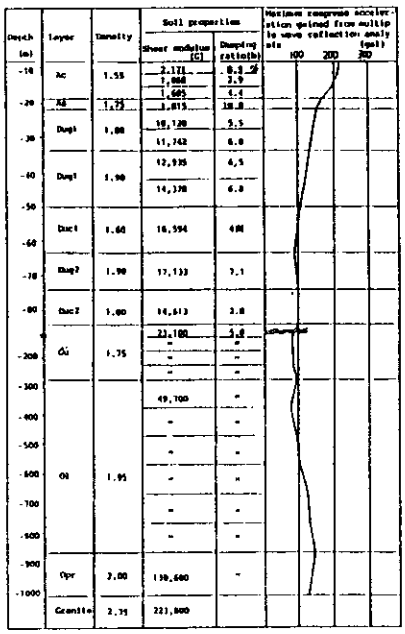

Figure 4. Multiple Wave Reflection Analysis of Deep Ground

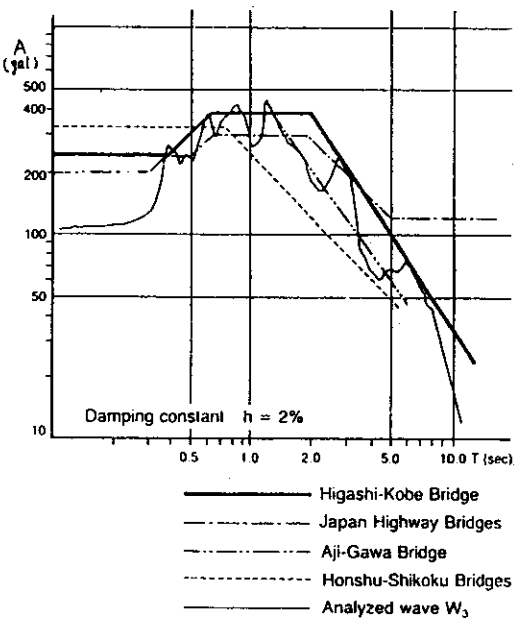

Figure 5. Design Acceleration Response Spectrum

As a result, the design acceleration at 4.4 seconds which corresponds to the natural period of the sway mode oscillation of the structure becomes 120 gal., which is nearly 1/3 of that used in standard bridges in Japan. The sectional forces and displacements using this design criterion have already been shown in Table 2.

Seismic forces taken into consideration were those from any direction that would trigger maximum stress on tower members, in addition to those applied longitudinally and transversely to the bridge. It was confirmed from a 1/100-scale full model vibration test that such stress

is the resultant of those caused by longitudinal and transverse seismic forces.

The design spectrum was confirmed by another study in which records by Japan Meteorological Agency Seismometer and the same records by SMAC were first compared to find differences in both waves and to find recording error of the SMAC. It was found that the error was caused by the spring which controls the SMAC pen movement. Since the ground moves slowly during a long period earthquake, the spring cannot have the power to pull the pen. The error which should be removed turned out to be the minimum value of the smoothed Fourier Spectrum. An attenuation equation was obtained from the relation between magnitude, epicentral distance and SMAC acceleration data modified by the above method. By supposing the Nankaido Earthquake that will cause the worst possible effect for the bridge site, the expected spectrum on the ground was obtained. As a result, it was found that the design spectrum already determined corresponds to the expected value of the mean plus 1σ (standard deviation) and was judged suitable for design use (Figure 6).

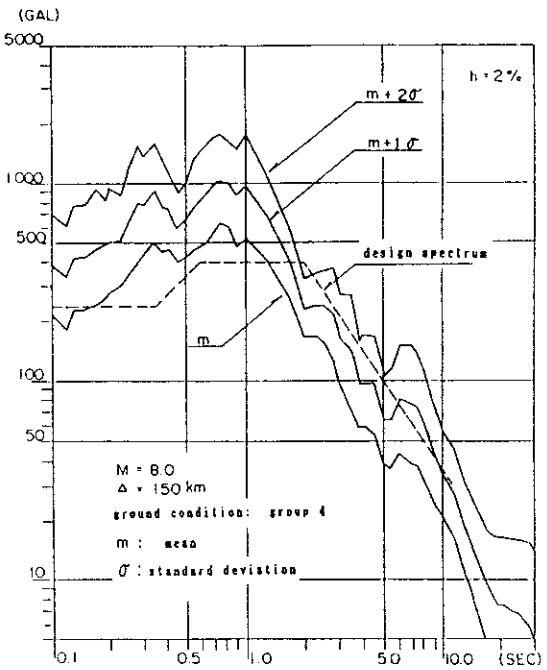

Figure 6. Confirmation of Design Spectrum

2.5. Earthquake Safety Devices — Development and Design

As there is not much data on earthquake resistant design for a cable-stayed bridge with a long natural period, it was decided to install vibration-resisting devices to prevent excessive girder movement which might result in tower collapse. A case in which a simple stopper is installed on each end pier was analyzed. The result indicated that because of the low rigidity of the piers, the movement of the heavy girders cannot be controlled.

After considering several devices, the vane-type oil damper was selected. The damper contains oil in its drum which is divided into two compartments. When the girder moves, the oil moves from one compartment to the next through an orifice in the partition. The turbulent flow generated when the oil passes through the orifice produces the power that moderates the girder movement (Figure 7). The characteristics of the vane-type oil damper are as follows:

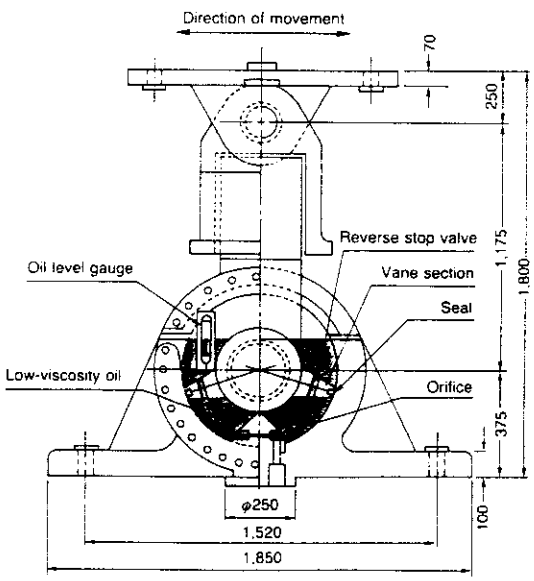

Figure 7. Vane-type Oil Damper

- The damper does not have the problem found in the case of simple stoppers in which small difference in clearance setting often results in big difference in reaction force.
- The effect of the damper increases as girder movement becomes larger and faster. This indicates that the damper is very effective in preventing excessive amplitude.
- The damper increases the safety margin without changing the characteristics of the natural period of the bridge.
- A well-designed damper reduces the girder movement and controls the reaction forces on the end piers.

Considerations for damper design and maintenance should include the following:

- There must not be a gap between the vane and the cylinder to prevent oil leakage.
- A dust cover is required to prevent oil contamination.
- The volume of the oil must be checked periodically.
- The effect of oil temperature on the damper performance is negligible.

To examine the characteristics and applicability of the damper, a 1/2-scale model was fabricated for performance testing. The test was conducted with different movement velocities and orifice sizes. The test results reveals that the turbulent flow resistance characteristic is given by the following expression:

$$F = 1840V^2 \times 2 \qquad \text{(in case the orifice angle is } 15°\text{)} \tag{1}$$

where V : girder movement velocity
F : resistance which is equivalent to the reaction on the pier.

In designing the damper, an earthquake that is 1.4 times stronger than that considered in the bridge design is assumed. Since the design spectrum corresponds to the expected value of the mean plus 1σ, the value of mean plus 2σ was considered to be suitable for design due to an unexpectedly strong earthquake. Using the characteristics of the vane-type oil damper and this earthquake input, nonlinear time history earthquake response analysis was conducted. The input earthquake used was that of the Izu Peninsula Earthquake.

Table 3. Effect of Vane-type Damper on Girder Displacement

Earthquake Level	Damping Constant (%)	Relative Girder Displacement (cm)	Maximum Response Velocity (cm/sec)	Damper Reaction (kN)
whole structure design level (1.0EQ)	2*	61*	—	—
	1	72		—
	2	61	98	—
	1+4.8**	48	75	1480
girder stopping device design level (1.4EQ)	1	102	231	—
	1+6.2**	64	99	3620

N.B. – Values marked with * were obtained using the design spectrum
– Damping constant marked with ** indicates damping of the whole structure plus damping due to the damper

The results are given in Table 3 and can be summarized as follows:

- If an earthquake 1.4 stronger than the design spectrum occurs on the bridge without the dampers (structural damping ratio of 1% is assumed), the displacement of the girder will be $72 \times 1.4 = 102$ cm. This will be over the critical displacement of 74 cm at which the tower buckles.
- If the dampers are installed, the girder displacement will be reduced to 64 cm, which is in the range of the design displacement of 61 cm. This is below the critical displacement for the tower to buckle. In this case, the equivalent damping constant due to the damper is calculated to be approximately 6% based on the displacement response.

2.6. Verification of Dynamic Behavior of the Bridge by Shaking Table Tests

The appropriateness of the method adopted to evaluate the bridge response to the earthquake and the effectiveness of the damper were confirmed by vibration tests using a three-dimensional 1/100-scale elastic model. The model was made of steel satisfying the similarity of stiffness and weight. The natural frequency and mode shapes of the model in several low modes agreed well with the analytically predicted ones. The structural damping of the model without the damper is adjusted to 1~2%, reflecting fairly light damping of a large flexible structure. An electro-magnetic damper is attached to the girder of the model to substitute the vane-type oil damper.

Modified long-period predominant and short-period predominant earthquake records were used for input earthquake ground motion. Results are shown in Table 4. All values are converted to the prototype for comparison. Displacement response due to the short period predominant earthquake (El Centro NS, 1940) record is found to be much less than the design values.

Table 4. Maximum Displacement Response (given in cm.) for Cases with and without Damper

Input Earthquake		Input Along Long'l Axis		Input Along Transverse Axis	
		Top of Tower		Girder Center	Top of Tower
		No Damper	W/ Damper	No Damper	W/ Damper
Long Period	Izu-oki Earthquake Synthesized Wave	64.0	50.0 (53.9)	65.0	56.0
	Chiba-oki Earthquake Corrected Wave	63.0	52.0 (51.6)	44.0	60.0
Short Period	El Centro Earthquake	18.5	17.0	35.0	30.0
Design Value by Response Spectra		60.4	—	79.4	82.0

N.B. – Tabulated values are corresponding to real bridge
– Viscous damping coefficient of 2% is assumed for cases without damper
– Values ( ) are those calculated from time history response analysis

Displacement response at the top of the tower due to the long period predominant earthquake motion without the damper is observed to be nearly equal to the design values. However, the energy dissipation of the damper suppressed the response fairly well to the design values. Close agreement of the experimental and numerically calculated results verifies both methods.

In addition to the above vibration tests, the following two tests were conducted. Recent earthquake observation in soft ground suggests long duration sinusoidal-type ground motion with relatively small amplitude. Hence, the frequency matched sinusoidal input motion with 10 gal (cm/sec^2) amplitude and 10 cycles are used for the resonance test of the model. The results shown in Figure 8 verifies that the damper is very effective in suppressing resonant-type response to one-third level.

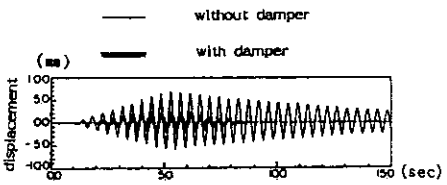

Figure 8. Effectiveness of Damper in Suppressing Resonant-Type Response

To investigate complex 3-D dynamic behavior of the bridge, single component vibration tests in three orthogonal directions and simultaneous three-component vibration tests were conducted and compared. Figure 9 shows the dynamic response of the bridge subjected to the motion in the EW (transverse) direction. From the results, it was confirmed that no interaction between the three directions exists. Comparing with the single component tests, it was found that 3-D results can be predicted from the linear superposition of the single component tests.

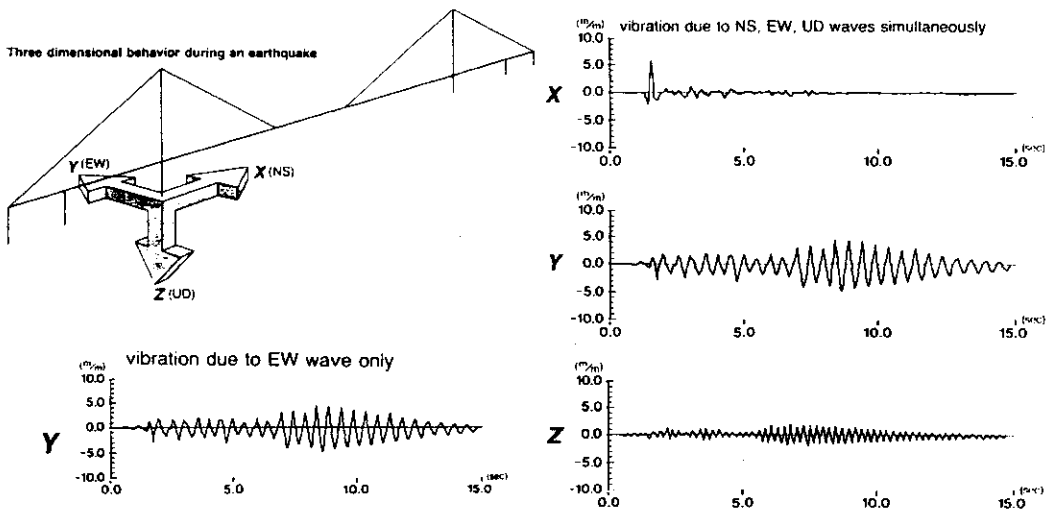

Figure 9. Three-Dimensional Behavior During Earthquake

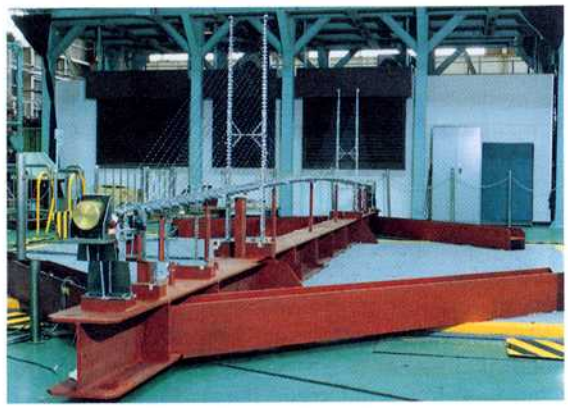

Figure 10. Full Model Vibration Test

3. WIND-RESISTANT DESIGN

3.1. General Concepts of Wind-Resistant Design of Higashi-Kobe Bridge

In the design of the Higashi-Kobe Bridge, it was considered that the bridge should not only satisfy its functional requirements but should also be aesthetically pleasing to the society as well. Two elegant straight columns tied at relatively low position were chosen for each tower of the cable-stayed bridge form in order to project its soaring image. For this reason, special considerations had to be taken in the wind-resistant design of the tower columns.

For the main girder, a truss structure was chosen to satisfy stability against wind from and to the Rokko Mountain adjacent to the bridge. Since vertical members are not used in the truss based on aesthetic point of view and the steel decks and the chord members used in the main girder are integrated on the same plane, the main girder was expected to behave as a double-wing system. Since elastic support system was designed along the bridge axis, the movement of the main girder and the bending of the towers due to wind had been investigated in detail.

A double-plane multiple cable system with harp pattern arrangement was chosen. Countermeasures to rain-wind induced vibration was adopted without sacrificing elegance.

Because of the unique configuration adopted for the Higashi-Kobe Bridge, wind-resistant design played an important role and was the critical factor in the design of the bridge.

3.2. Wind Observation

(1) Fundamental Wind Velocity

The fundamental wind velocity (the expected value of 10-minute mean wind speed for 100-year return period at the height of 10m) was estimated by the Gringorten method and multiple regression method with the topographical factors. The results were 38.3m/sec and 37.5m/sec, respectively. The fact that the wind speeds at the bridge site were almost 1.2 times

than those at the Kobe Marine Meteorological Observatory was also taken into account. With reference to the fundamental wind speed of 43m/sec specified for the Akashi Kaikyo Bridge, the fundamental wind speed for the Higashi-Kobe Bridge was specified at 40m/sec. The characteristics of natural wind at the bridge erection site was analyzed using data obtained from a 50m wind observation tower, which was built for this purpose.

(2) The Inclination of Wind

Wind recordings taken by ultrasonic anemometer have revealed that:

- In general, wind blows upward in the low-wind speed range due to the effect of Rokko Mountains, but level in high-wind speed range.
- In the wind speed range of 10–20m/sec, the inclination of wind is $+2°$ on the average. As the fluctuating inclinations (3σ of 30-second moving average) were found to be $\pm 6°$, it have been decided to set the maximum inclination at $\pm 8°$ for upward flow and $-6°$ for downward flow for safety consideration in low-wind speed range (Figure 11).

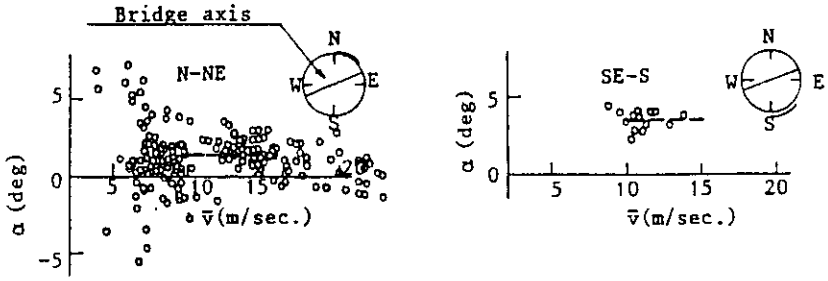

Figure 11. Observed wind inclination at the site

3.3. Stabilizing Countermeasures for Wind Action

3.3.1. Main Girder

As a truss-type frame is employed for the main girder, the Higashi-Kobe Bridge is relatively stable from aerodynamic point of view. However, it is not always free from vortex-excited flexural oscillation or torsional flutter. Also because of the all-free supporting system, it is important to investigate the wind response along the bridge axis.

(1) Vortex-Induced Vibration and Flutter

The wind tunnel tests were carried out using a two-dimensional 1/28 scale model. Natural frequencies of deflection and torsion of the prototype are 0.42 Hz and 1.13 Hz, respectively. Solidity ratio is 0.41.

The Higashi-Kobe Bridge, with a truss girder having a small solidity ratio, is less subject to vortex-induced oscillation. The bridge stability against self-excited and divergent oscillation such as torsional flutter was proved to be sufficient in wind tunnel tests (Figure 14). The aerodynamic stability of the main girder was also checked in wind tunnel tests using a model of the entire bridge with the towers and cables installed (Figure 12).

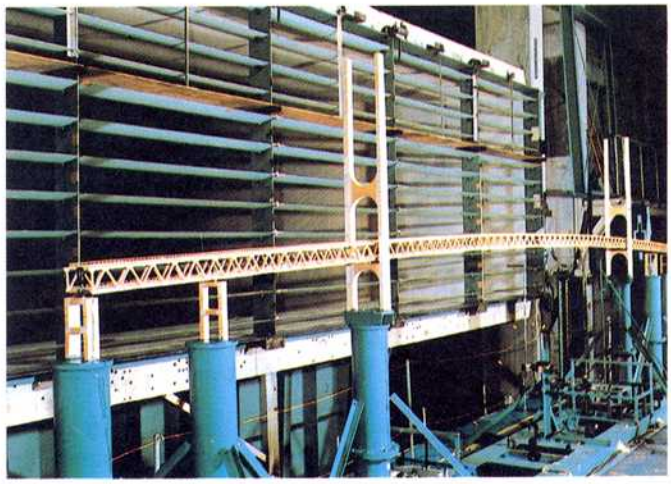

Figure 12. Wind tunnel test for girder and tower $\eta = 1/100$

(2) Buffeting Response

Because the steel deck and chord members used in the main girder are integrated on the same plane (Figure 13), the area exposed to wind is smaller than if they were mounted on the cross beams, resulting in reduced drag ($C_D = 1.3$). The double-wing shape of the main girder increases the lift derivative with angle of attack ($dC_L/d\alpha = 12.7, \alpha = -2° \sim +3°$), suggesting the possibility of large buffeting response amplitude. The buffeting response was studied by wind tunnel test and also by response analysis in which on-site turbulence characteristics were taken into considerations.

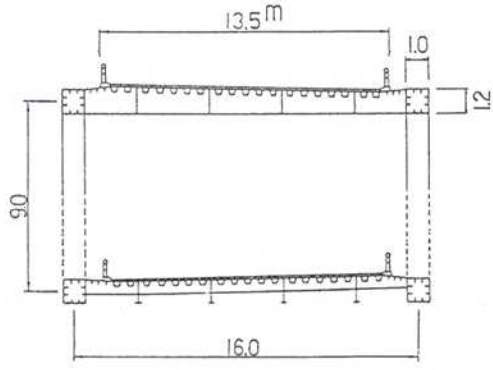

Figure 13. Double-Wing shape of Main Girder

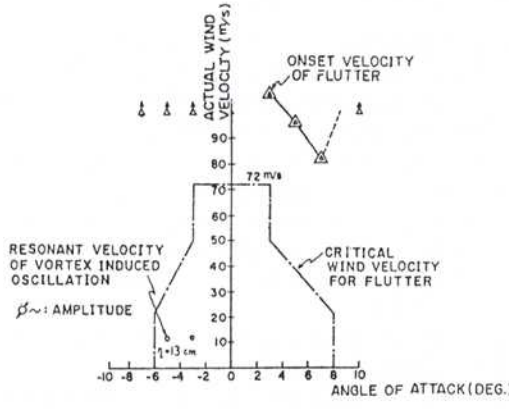

Figure 14. Stability against Vortex-induced Vibration and Flutter (Uniform Flow)

Using an entire model of the bridge, response in turbulent flow was studied by varying the scale and intensity of turbulence. Figure 15 shows the aerodynamic admittance obtained from the results.

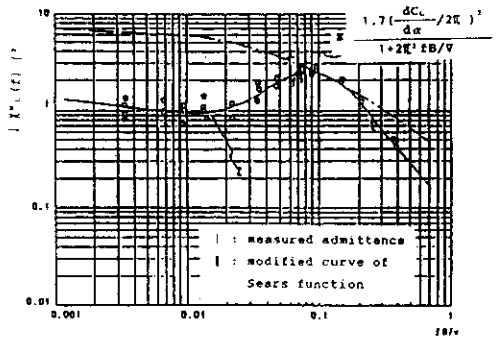

Figure 15. Aerodynamic Admittance

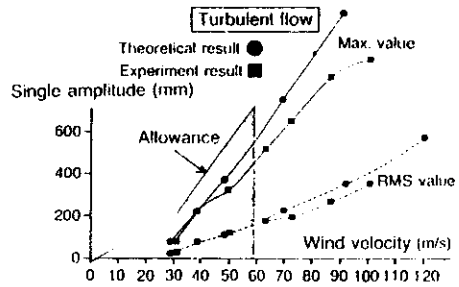

Figure 16. Buffeting Response to natural wind

Figure 16 shows the actual bridge buffeting response amplitude obtained from the admittance under the exposure to natural wind prevailing at the site. These values are within the allowable amplitude which have been determined from the fact that there is no live load when strong wind blows and that there is still room for yield point for the oscillation. Safety against fatigue is also examined. The bridge resistance against buffeting is satisfactory.

Although the experimental data and calculated data exhibit a relatively high degree of agreement in the low wind velocity region, the calculated data are shown to somewhat exceed the experimental data as the wind velocity increases (Figure 16). This is probably because the influences of aerodynamic forces acting on the towers, cable, etc., or the oscillation in the direction of wind axis were considered when the wind velocity increases.

As it is clear from the above, it can be said that the amplitude of buffeting response of the entire bridge structure is generally determinable when analyzed by the quasi-steady theory employing the static aerodynamic coefficient.

(3) Longitudinal Response due to static and gust effect

Since the structural system of the Higashi-Kobe Bridge is of all-movable type and it has diagonal members, the girder can be moved by an oblique wind along its longitudinal axis. This necessitates a close look at the displacement of the main girder including gust effect. Therefore, a gust response factor was determined by Davenport's method and used in the analysis. In the analysis,

- only the primary vibration mode was used,
- the length for calculation of 885m was taken as the total length of the bridge,
- roughness coefficient of ground surface K_r was set to be 0.005 and decay factor k to be 10.

As a result, gust response modification factors ν_2 and ν_4 to be used in design have been determined as follows:

$\nu_2 = 1.20$: modification factor for fluctuating wind speed on time and space,

$\nu_4 = 1.25$: modification factor for dynamic response of the structure.

3.3.2. Tower

(1) Countermeasure against galloping

The upper crossbeam is located at relatively low position. The very long free-standing portion can easily experience wind-induced vibration within a tower plane. To study the tower column (3.5m×4.5~6.5m) stability, wind tunnel tests were conducted. Figure 17 shows the

cross sectional shapes of 2-D models. The size of square corner-cut, expressed as the ratio of corner cut length a to model depth D, was varied from $a/D = 0$ (original rectangular cross section with slenderness ratio $B/D = 1.46$) to 6/18 with an increment of 1/18.

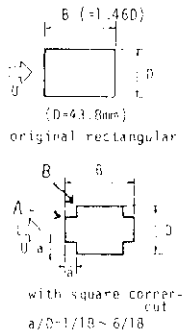

Figure 17. 2-D Models

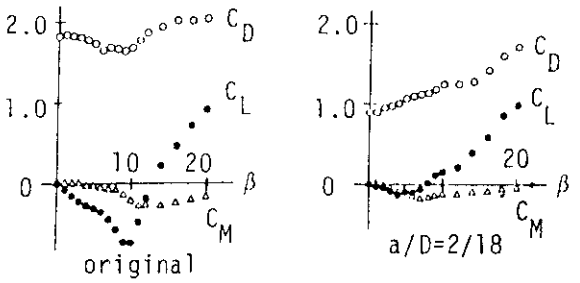

Figure 18. Aerostatic force coefficients of 2-D prisms

Aerostatic forces (C_D, C_L, C_M) against the incident angle of air flow β, are shown in Figure 18. When $a/D = 2/18$ and $3/18$, the value of C_D is only half that of C_D in the original rectangular cross section. Simultaneously, the absolute value of the increment of C_L at $\beta = 0°$ and the minimum value of C_L seem to be significantly reduced.

Flow patterns around a stationary model at $\beta = 0°$ are shown in Figure 19. In the case of the original rectangular section $(a/D = 0)$, separated shear layers appear considerably closer to the body side surface and form a rather narrow wake, in which the separated shear layer seems to reattach itself near or at the leading edge B. Then, further increase of a/D from $a/D = 4/18$ on leads to re-separation from the leading edge B.

Figure 19. Flow patterns around stationary 2-D prisms

Vibrational responses of these 2-D models are shown in Figure 20. As shown in these figures, the galloping characteristic depends on the size of corner cut in the same way as the aerostatic properties. For the original rectangular cross section, the vibrational amplitude begins to diverge at a reduced velocity $V_r = 8$. However, if $a/D = 2/18$, the critical flow velocity of galloping oscillation V_r increases to $V_r = 25$.

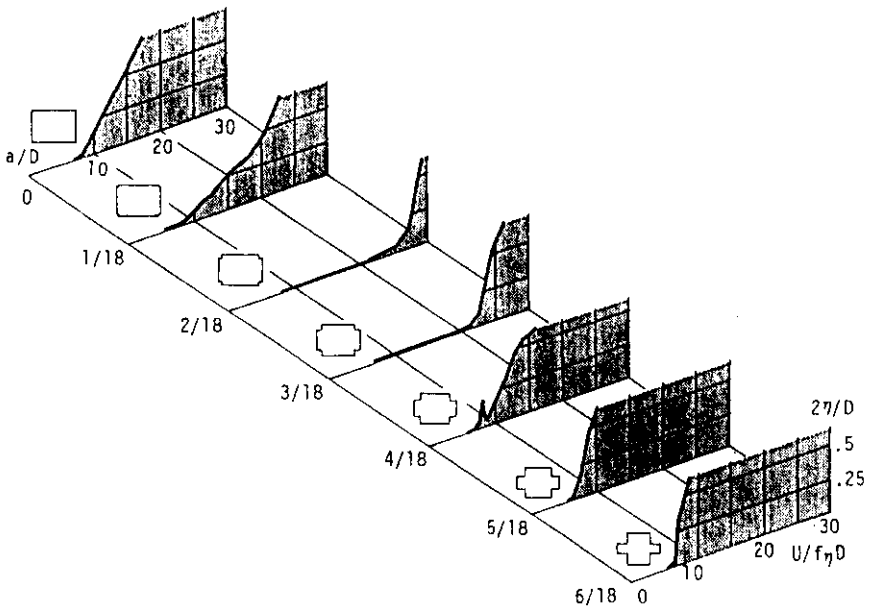

Figure 20. Aerodynamic vibrational responses of 2-D prisms with various size of square corner-cut

To confirm this effect, 3-D wind tunnel test was conducted using a 1/100 scale model. The test results showed that the galloping within a tower plane could occur at a relatively low wind velocity of approximately 20m/s. Cuts on each corner equal to about 10% (40cm × 40cm) of the tower front width was an effective solution (Figure 21). To obtain the corner-cut shape, cover plates are attached to the front and back of the column (Figure 22).

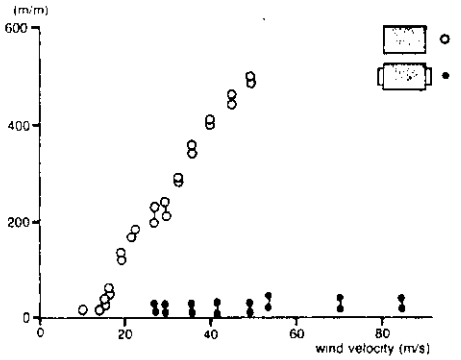

Figure 21. Aerodynamic Response of Tower

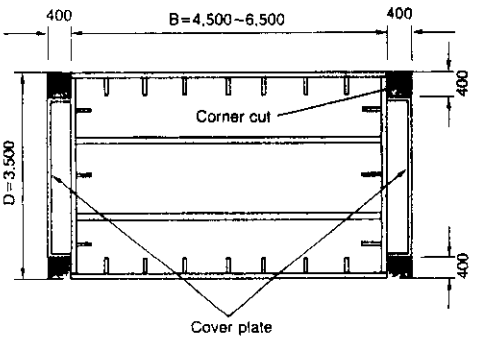

Figure 22. Cover Plates to Counter Vibration

(2) Stability during Construction

The main obstacle to safety during construction is the wind, which can also hinder the construction work. A model of the bridge under construction at the stage when the main girder cantilevering is in progress was tested (Figure 23). The test results show that buffeting would occur on the main girder during cantilevering as would the complete bridge, but that it would not be large enough to cause problems. However, in the construction stage when the towers are not supported by cables and the protective net around the tower used to catch

falling objects is not in place, rather large vortex-induced oscillation would be expected when the bridge is subjected to wind blowing transversely (Figure 24). To counter this, a tuned mass damper was installed on the top of each tower.

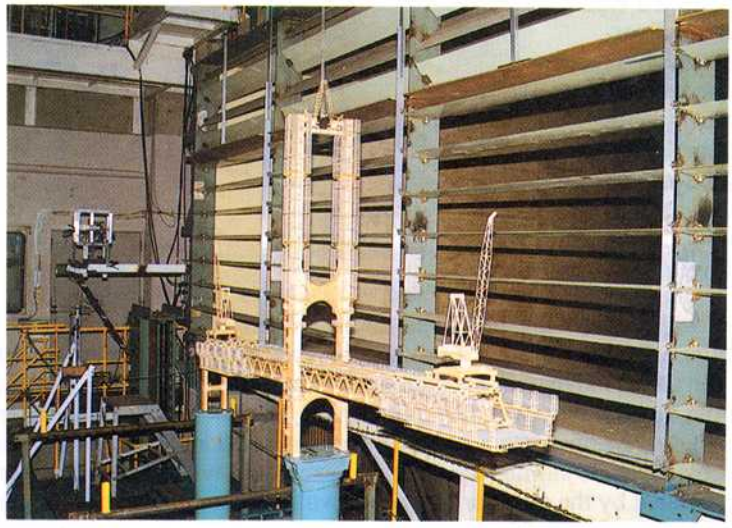

Figure 23. Wind Tunnel Test on Tower During Erection Stage

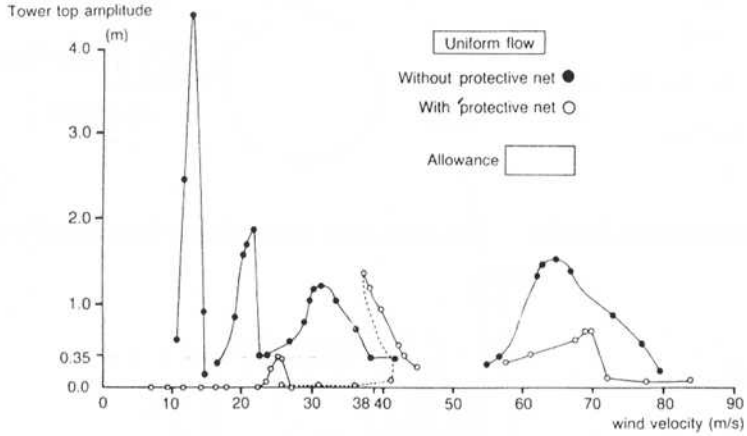

Figure 24. Out-Plane Response of Free-Standing Tower

3.3.3. Cables

Rain-wind induced vibration of polyethylene-lapped multicables have often been reported on other bridges. Rain-wind induced vibration of cables is influenced by various factors such as cable attitude of cable-stayed bridge, cable surface material, surface water repellence, cable dynamics, cable diameter, rain intensity, wind direction, wind speed, turbulence of wind and so on. Furthermore, these are summarized to the direct influential factors to cable

aerodynamics such as Reynolds number, formation of water rivulet on cable surface, Scruton number, cable vibrating mode, cable relative attitude to wind.

Rain plays an important role for cable excitation in formation of water rivulet. Rain can make the inclined cable model aerodynamically unstable. On the other hand, the rough surface cylinder lapped by wire netting is stabilized by changing its velocity diagram from a divergent flutter type to a restricted type. Yawed circular cylinder shows divergent cross-flow oscillation, which is similar to galloping, even without rain. Yawed circular cylinder shows only unstable buffeting and/or rolling oscillation for small yawing angle from 0° to 22.5° and stable cross-flow oscillation for larger from 25° to 45° in the range from 0° to 45°, respectively (Figure 25).

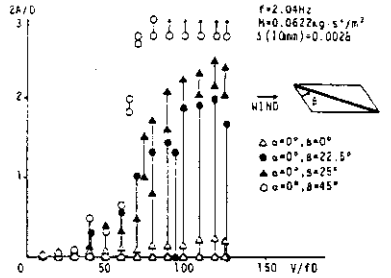

Figure 25. Effect of Yaw Angle β on Response

The intensive axial flow in the near wake of yawed circular cylinder with $\beta = 45°$ can be visualized as shown in Figure 26 (by tiny flag installation). This axial flow is considered to be extremely important for the aerodynamic excitation of yawed/inclined cable. This is similar to the aerodynamic role of axial flow with the splitter plate, in which cross flow flutter is excited for a circular cylinder submerged into a wake of circular cylinder (Figure 27). This phenomenon was confirmed by the quite similar aerodynamic excitation with yawed cylinder by the artificial axial flow generated by the peculiar device shown in Figure 28, of the circular cylinder normal to flow as shown in Figure 29.

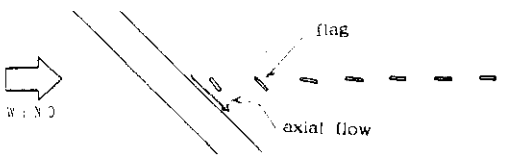

Figure 26. Flow Pattern behind Yawed Circular Cylinder

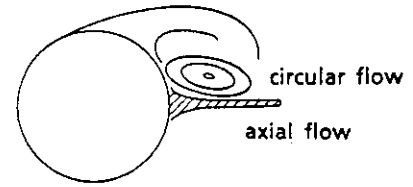

Figure 27. Axial Flow and Inner Circulatory Flow

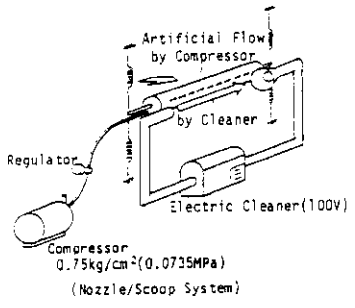

Figure 28. Device for Artificial Axial flow

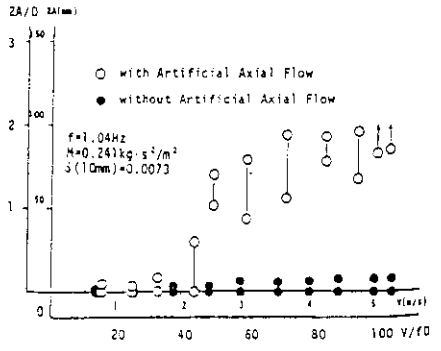

Figure 29. Cross-Flow Response Diagram of Circular Cylinder with Artificial Axial Flow in its Wake

Figure 30 shows that there are two different characteristics boundaries between aerodynamic stability and instability. These are the mean velocity V_a and the r.m.s. value of the flow in near wake. Aerodynamic instability could occur when both conditions that V_a and r.m.s. value are larger and smaller than 55% of approaching velocity V and 25% of mean velocity V_a, respectively, are satisfied.

Finally, using wind tunnel tests of a cable (Figure 31) with actual weight and length of 10 meter, the vibration mechanism was confirmed to develop a counter-vibration measure. As mentioned above, the vibration is caused by air flow created around each cable by the winds blowing diagonally across the cable axis. The vibration is aggravated by rain. Raindrops on the upper surface of a cable do not run around the circumference because of the diagonal wind force, but form a rivulet along the cable. This could become a separation point of the wind and would cause strong inner circulatory flow.

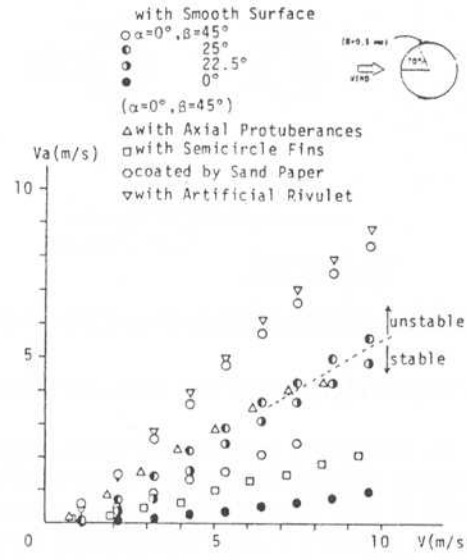

Figure 30. Axial Flow Velocity in near wake of yawed Circular cylinder and aerodynamically stable/unstable boundary

It was found that attaching protuberances (Figure 33) parallel to the cable axis would be effective in controlling the vibration (Figure 32), since those protuberances prevent rain from forming a rivulet and actual cable has some 0.01 logarithmic damping. Stability of these section without rain has also been confirmed. The developed cross section of the cable has double polyethylene layers. Outer one is to form a gear-like section. Inner one is to protect wires from rusting. The purpose of the double tube structure is to prevent crack propagation at the surface of the inner one even if crack occurs during erection.

Figure 31. Wind Tunnel Test for Cables

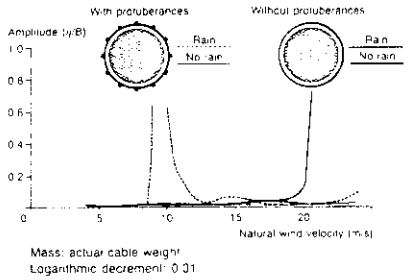

Figure 32. Aerodynamic Response of Stay Cable

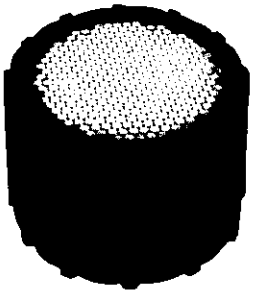

Figure 33. Cross Section of Cable showing double polyethylene layers

4. VIBRATION TEST OF THE ACTUAL TOWERS

In earthquake resistant and wind stability design process of the Higashi-Kobe Bridge, damping characteristics of the tower itself is assumed as $h = 0.01 \sim 0.02$ (damping ratio) and $\delta = 0.01$ (logarithmic decrement), respectively. It is noted that there exists the well-known relation $\delta = 2\pi h$. Those values are adopted based on previous design practices when relatively large damping capacity is expected due to large amplitude of vibration due to severe earthquake excitation.

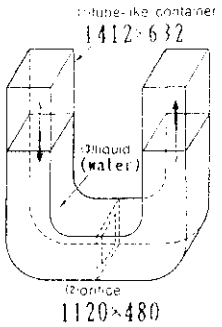

Figure 34. Tuned Liquid Column Damper

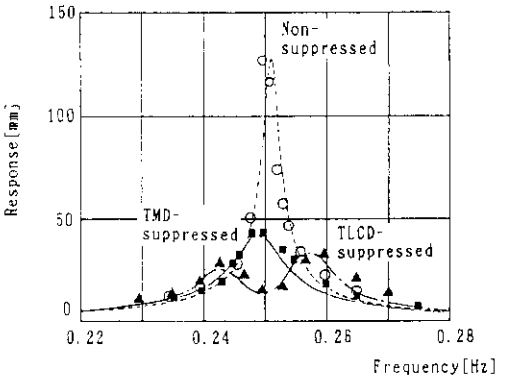

Figure 35. Resonance Tests

Table 5. Natural frequencies and Damping Capacity of the Towers

Mode	Frequency (cps)	Logarithmic Decrement		
		Tower only	with TMD	with TLCD
1st	0.256 (0.249)	0.028 ~ 0.040	0.098	0.110
2nd	1.107 (1.050)	0.094 ~ 0.099	—	—

* Values in () obtained by analysis

Vibration experiments of the actual tower of the Higashi-Kobe Bridge using a pair of exciters were employed to verify the dynamic property assumed in the design and the efficiency of the vibration suppressing devices used only during construction, namely TMD (Tuned Mass damper) and TLCD (Tuned Liquid Column Damper) as shown in Figure 34. The exciters and the dampers were attached to the top of the tower.

The natural frequency and damping of the tower are shown in Table 5. Calculated and measured natural frequency agrees fairly well in 1st and 2nd modes. The logarithmic decre-

ment was found to be about 0.03 for the first mode without dampers.

The frequency response curves of the tower with and without dynamic dampers are shown in Figure 35. The maximum response of the TMD– and TLCD–suppressed cases are reduced to almost 1/3 of that of non-suppressed case. It is verified that logarithmic decrements of those devices are more than 0.1 and effective to control vortex-induced excitation.

5. CONCLUSIONS

Main conclusions obtained in this study on aseismic and wind-resistant design of the Higashi-Kobe Bridge are as follows:

- The main girder is supported by the towers through cables in such a way that the girder is movable in the longitudinal direction. By this supporting method, the fundamental period of the bridge is lengthened to reduce seismic design forces. Consequently, the size of the foundations of the tower was significantly reduced.
- To avoid large displacement due to the all-free girder supports, harp pattern arrangement of the cable was adopted. In addition, harp pattern is considered to be aesthetically favorable due to no visual criss-crossing of the cables when viewed from the sides.
- To prevent failure of the towers due to excessive displacement by exceptionally large earthquake ground motion, vane-type oil damper has been developed and installed between the main girder and the end piers.
- The two projecting columns were adopted for aesthetic reasons. To avoid galloping of the towers, the corners of the section of the tower were cut.
- To prevent wind and rain-induced vibration of the cables, gear-like section for cables has been developed and is the first time to be used in the world.
- Because high sensitivity was observed in the buffeting response of the girder with the upper and lower deck plates, safety against vibration was experimentally and analytically confirmed.
- In estimation of longitudinal displacement due to wind, fluctuating response due to gust effects has been considered in addition to the static loads.

6. REFERENCES

1. Toki and Nakase [1986]: "Reliability of Long Period Component of SMAC Accelerograms," *Proc., 7th Japan Earthquake Engineering Symposium.*
2. Kitazawa, Ishizaki, Emi, and Nishimori [1990]: "Characteristics of Earthquake Responses and Aseismic Design on the Long-Period Cable-Stayed Bridge (Higashi-Kobe Bridge) with All Movable Shoes in Longitudinal Direction," *Proc., Japan Society of Civil Engineers,* 422.
3. Kitazawa, Noguchi, Nishimori, Izeki [1991]: "Earthquake Resistant Design of a Long Period Structure and Development of Girder Displacement Stopper (Higashi-Kobe Bridge)," *Innovations in Cable-Stayed Bridges.*
4. Saito, Shiraishi, and Ishizaki [1988]: "On Aerodynamic Stability of Double-Decked Trussed Girder for Cable-Stayed Higashi-Kobe Bridge," *International Colloquim on Bluff Body Aerodynamics and Its Applications.*
5. Shiraishi, Matsumoto, Shirato, and Ishizaki [1987]: "On Aerodynamic Stability Effects for Bluff Rectangular Cylinders by Their Corner-Cut," *Proc., 7th International Congress on Wind Engineering.*
6. Matsumoto, Shiraishi, Shirato [1991]: "Rain-Wind Induced Vibration of Cables of Cable-Stayed Bridges," *8th International Conference on Wind Engineering.*